Electron spin resonance–scanning tunneling microscopy experiments on thermally oxidized Si(111)

Y. Manassen, E. Ter-Ovanesyan, D. Shachal, and S. Richter
Department of Chemical Physics, The Weizmann Institute of Science, Rehovot 76100, Israel
(Received 16 March 1993)

In this paper several electron spin resonance–scanning tunneling microscopy (ESR-STM) experiments are described. In this technique, the tip of a STM scans a surface that contains isolated paramagnetic spin centers. The individual spin centers apply a time-dependent perturbation on the tunneling electrons, giving rise to a time-dependent component of the tunneling current—at the Larmor frequency [$J(\omega_L)$]. This occurs only when the tunneling region is close to the spin center. Therefore, $J(\omega_L)$ is spatially localized. Reproducibility of the spatial localization together with a reproducible tip-dependent frequency shift were observed. In higher magnetic fields the average linewidths, together with the fluctuations in the frequency of the signal (probably due to the electric fields near the spin center), are larger. The proposed mechanism is that electric-dipole-moment oscillations, which are modulated by the Larmor frequency (the Zeeman effect), will give a significant $J(\omega_L)$ component close to the tunneling region by modulating both the barrier height and width.

The scanning tunneling microscope[1,2] (STM) is a revolutionary device that is capable of atomic resolution. It can provide information on conducting surfaces, either semiconductors or metals.[2–8] Studying local physical phenomena[9–13] is also possible and an example is the observation of the precession of individual paramagnetic spins with the use of[14–17] electron spin resonance–scanning tunneling microscopy (ESR-STM). In this technique, weak rf signals—at the Larmor frequency—are observed. In order to detect these weak rf signals a home-built ultrahigh-vacuum scanning tunneling microscope with a highly sensitive rf system was constructed. This system includes a network for impedance matching, an rf amplifier, and a spectrum analyzer. In order to detect the expected signal intensities, an extremely small bandwidth, together with a low noise detecting system must be used. Our best noise level is -160 dBm (at a bandwidth of 10 Hz), which means that signal levels of a little less than 0.1 nA are still detectable. Most of our experiments were done on thermally oxidized Si(111) surfaces. Such surfaces, because of the lattice mismatch between silicon and silicon dioxide, contain unoxidized paramagnetic silicon dangling bonds (one out of 1000 surface silicon atoms)—P_b centers.

The initial experiment was done in a field of 139 G which was measured by a Gaussmeter. The predicted Larmor frequency was 389.2 MHz. Two examples of the observed spectra are shown in Figs. 1(a) and 1(b). The detection bandwidth was 100 Hz. The peaks have a linewidth of 200–400 kHz, and show a change in the frequency of 2 MHz.

In order to demonstrate the dependence of the detected signal on the magnetic field and to check whether signals are detectable only at the Larmor frequency, the field was increased to 157 G (where the Larmor frequency is expected to be 439.6 MHz). Several experiments were done with a much larger spectral width. An example is shown in Fig. 1(c). The linewidth of this peak is broader than in Figs. 1(a) and 1(b). This might be due to the fact that the signal is smeared by a too rapid sweeping. Nevertheless, the signal was found only at a frequency of 437.5 MHz. In all these experiments, the signals are observed at the Larmor frequency but have some random frequency shift of about 3–4 MHz [such as in Figs. 1(a) and 1(b)].

In order to demonstrate spatial localization, a computer program which records rf spectra from several close (3 Å apart) locations on the surface was written. A two-dimensional map is observed, in which the horizontal axis displays the rf spectrum and the vertical one, the spatial location on the surface. Examples are shown in Fig. 2. The rf signal is observed over a spatial range of 10 Å on the surface. The spatial localization of the signal is reproducible. The spectra shown [in Figs. 2(a)–2(d)] demonstrate that in four consecutive attempts the signal appeared at the same location on the surface, namely, it is possible to return to the same location on the surface and to see the signal again. This reproducibility demonstrates the validity of the ESR-STM technique. It will enable more systematic studies on the same spin center.

Although the shape and the central frequency of the peak are subject to random variations, the signal observed at larger spatial coordinate [higher in the sequence

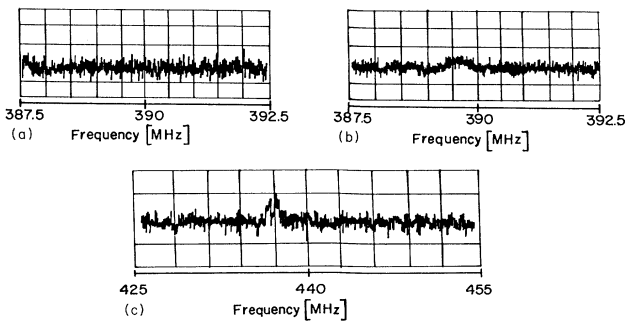

FIG. 1. rf spectra of the tunneling current in a magnetic field of 139 G [(a) and (b)] and 157 G (c). Notice that the span width in (c) is much larger.

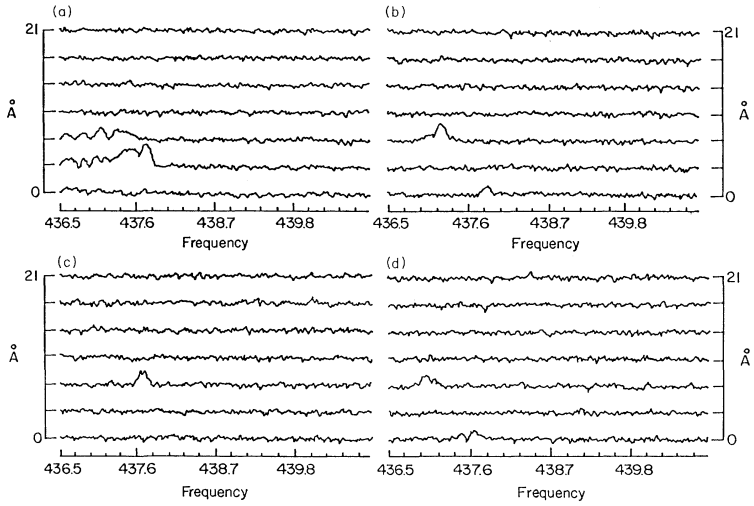

FIG. 2. rf spectra of the tunneling current at a field of 157 G. The horizontal axis displays the frequency and the vertical one the spatial location on the surface. The distance between two consecutive (vertical) spectra is 3 Å. (a)–(d) show four consecutive spatially dependent rf spectra of the tunneling current at the same locations on the surface. These spectra demonstrate the reproducibility of the spatial localization, as well as the reproducibility of the spatially dependent frequency shifts. Frequencies are measured in MHz.

in Figs. 2(a)–2(d)] is at a slightly lower frequency than the other one. This shift is reproducible, and is observed in three consecutive spectral sequences [Figs. 2(a), 2(b), and 2(d)]. This demonstrates a certain correlation between the rf signal and the spatial location. This is probably due to electric fields which are dependent on the relative orientation between the tunneling region and the spin center.

Further increasing the field to 250 G gives a signal at 700 MHz. According to our results so far [Figs. 3(a) and 3(b), for example], at this frequency the lines are broader (2–5 MHz) and their frequency fluctuations are stronger. Of course, this reduces the signal intensity and makes it harder to detect. In order to make the signal clearer, a low-pass Fourier filter was applied on the spectra. This phenomenon might be due to genuine relaxation processes which are more effective at higher frequencies, or due to increased dephasing due to the interaction with the tunneling electrons. This question will be investigated.

It will be shown that these observations are consistent with a mechanism of modulation of the tunneling probability at ω_L when the tunneling electrons are in close proximity to a spin center which exhibits the Zeeman effect. In order to show this a detailed calculation was done on a relevant model which represents the P_b center.[15,16]

Conventional ESR studies on thermally oxidized Si(111) surfaces gave a g anisotropy of ~ 0.01.[18] The anisotropy of the g tensor is due to the contribution of orbital angular momentum to the total one. The spin angular momentum gives a fully isotropic g value. Therefore, the size of the anisotropy provides the size of the effective orbital angular momentum. The first approximation which is made, in order to develop a model for the g anisotropy of the P_b center, is looking only at the defect "molecule." The structure of a silicon crystal is a diamond lattice, in which each atom is bonded to four nearest-neighbor silicon atoms. Due to the tetrahedral symmetry, the basic electronic functions are the $|SP^3\rangle$ functions. The basis functions are, thus, $|SP_0^3\alpha\rangle, |SP_0^3\beta\rangle, \ldots, |SP_3^3\beta\rangle$ (including the spin functions). The coordinate system is chosen such that the $|SP_0^3\rangle$ orbitals are in the (111) direction (normal to the surface). It is higher in energy by Δ. The additional term in the Hamiltonian is the spin-orbit coupling λLS, where λ is the spin-orbit coupling constant, and L and S are the orbital and spin angular momenta, respectively. After that the Zeeman term is added (in the presence of the magnetic field): $\beta(L+g_eS)H$ where β is the Bohr magneton and H is the external magnetic field. g_e is the "free" spin g value. Diagonalization gives the g value of the ground-state Zeeman transition. It is found that when the magnetic field is parallel to the dangling bond, $g=g_e$. When the field is perpendicular to it, $g=g_e+\lambda/\Delta$. Comparing this with the experimental g values gives $\lambda/\Delta \sim 0.01$.[15,16] The spin-orbit coupling regenerated the "quenched" orbital angular momentum to the size of λ/Δ.

As is known from inelastic tunneling spectroscopy, the

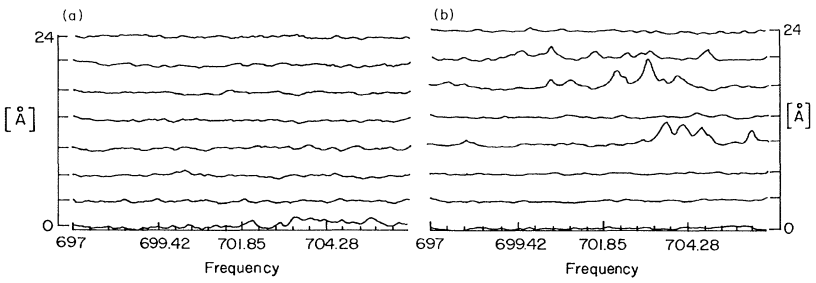

FIG. 3. Two spatially dependent rf spectra (not of the same location) showing the larger linewidths and the larger frequency shifts of the signal at higher magnetic fields (250 G). Frequencies are measured in MHz.

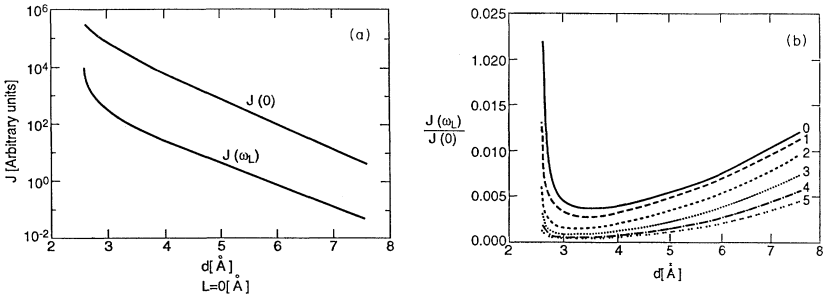

FIG. 4. (a) The calculated intensities of the time-independent $[J(0)]$ and the Larmor frequency $[J(\omega_L)]$ components of the tunneling current for different tunneling distances d. (b) The ratio $J(\omega_L)/J(0)$ as a function of d for several lateral distances (parallel to the surface). The lateral distance L in Å is written at the right side of each curve (the numbers 0,1,2,3,4,5).

tunneling electrons are capable of exciting different modes in tunneling junctions. It is clear that the presence of an electric dipole moment in the spin center implies a nonzero transition probability between the states, which means that for a certain orientation between the tunneling electrons and the spin center, a steady superposition of electronic states will arise. Calculating this superposition is a tedious theoretical problem and therefore certain excited states were assumed *a priori*.[16] The charge density in $|SP_0^3\rangle$ (which has the largest interaction with the tip) is time dependent, and this time evolution is modulated by the Larmor frequency, namely,

$$\rho_{|SP_0^3\rangle}(t)=a_0+\sum_n a_n\cos(\omega_L T/2)\cos(\omega_\Delta t)\ ,$$

where $\omega_\Delta\approx\Delta/\hbar$. The maximum size of the sum of the ω_L modulated components $(\sum_n a_n)$ is approximately λ/Δ, which is the size of the effective orbital angular momentum. These results are quite general. Namely, the size of the g anisotropy will give the size of the Larmor frequency modulated component. The difference frequency is the Larmor frequency ω_L. The ability to observe difference frequency components with the STM was demonstrated in several different experimental systems.[19,20]

The question which now arises is how the oscillating charge density $[\rho_{|SP_0^3\rangle}(t)]$ affects the elastic tunneling process in close proximity to the spin center and what is the relative size (to the dc component) of the Larmor frequency component of the tunneling current $[J(\omega_L)/J(0)]$. An order-of-magnitude answer is provided by the following crude calculation: The most important interaction between the spin center and the tunneling electron is Coulombic (e^2/r). The time-dependent Coulombic interaction as a result of the charge-density oscillation can be described as the following: $E_{se}=0.01(e^2/r)\cos(\omega_L t/2)\cos(\omega_\Delta t)$, where 0.01 is the relative amplitude of this oscillating component. Using conventional units, $E_{se}(t)$ can be written as $\{0.14\ \text{eV}/r[\text{Å}]\}\cos(\omega_L t/2)\cos(\omega_\Delta t)$. r is best approximated as $\sqrt{L^2+(d/2)^2}$, where L is the lateral distance between the spin center and the tunneling electron and d is the tunneling distance. In the STM, at a large tip-sample distance, the barrier height is an average between the work functions of the tip and the sample (V_∞). As the barrier width is reduced, the effective barrier height (V_e) becomes smaller according to the formula $V_e=V_\infty-\alpha/d$, where $\alpha\sim 10$ eV Å.[21] The effective time-dependent barrier height will be $V_e(t)=V_e+E_{se}(t)$. Since the barrier height and width are connected it is possible to write $d(t)=\alpha/[V_\infty-V_e(t)]$, namely, a time-dependent barrier width is observed. The time-dependent tunneling current is $J(t)\simeq e^{A\sqrt{V_e(t)}d(t)}$, where $A=\sqrt{(8\pi m/\hbar)}$. The calculation is completed by a Fourier transform of $J(t)$ and finding the ratio $J(\omega_L)/J(0)$ [$J(0)$ is the time-independent tunneling current]. The fact that $\rho_{|SP_0^3\rangle}(t)$ is affecting both $V_e(t)$ and $d(t)$ gives a rather strong time-dependent tunneling current. Due to the extreme nonlinear nature of $J(t)$, a significant $J(\omega_L)$ component is observed. Figure 4(a) shows the intensities of $J(0)$ and $J(\omega_L)$. Figure 4(b) shows the ratio $J(\omega_L)/(0)$ at several d and L, showing the expected spatial localization. The calculated intensities are 10–30 % of the observed ones. A more accurate calculation must be performed to clarify this point.

ESR-STM was also used to observe a large free radical molecule deposited on a gold surface. The observed signal was weaker (few picoamperes) than on P_b centers and a special lock-in detection system was required.[17] This is consistent with the proposed mechanism due to the smaller size of effective orbital angular momentum of this molecular spin center.

The spin center which was examined with the STM is influenced by strong electric fields. These fields are expected to change the size of the effective orbital angular momentum (λ/Δ). The mechanism predicts that an increase in the frequency of the signal (larger λ/Δ) as a result of different electric fields (for example, due to different tip locations) have to be associated with an increase of intensity. Such behavior is observed in most [Figs. 2(a) and 3(b) and 3(c), for example] but not all [Fig. 2(b)] spectra.

An alternative mechanism was proposed.[22] Although several facts support the mechanism described here, further studies are required to clarify the correct mechanism.

This work was done under partial support of the U.S.-Israel Binational Science Foundation and of the Basic Research Foundation administered by the Israeli Academy of Science. We would like to express our gratitude for additional assistance of the Glickson Fund.

[1]G. Binnig, H. Rohrer, Ch. Gerber, and E. Weibel, Phys. Rev. Lett. **49**, 57 (1982).
[2]G. Binnig, H. Rohrer, Ch. Gerber, and E. Weibel, Phys. Rev. Lett. **50**, 120 (1983).
[3]V. M. Hallmark, S. Chiang, J. F. Rabolt, J. D. Swalen, and R. J. Wilson, Phys. Rev. Lett. **59**, 2879 (1987).
[4]M. D. Pashley, K. W. Haberen, W. Friday, J. M. Woodal, and P. D. Kirchner, Phys. Rev. Lett. **60**, 2176 (1988).
[5]R. S. Becker, J. A. Golovchenko, E. G. McRae, and B. S. Swartzentruber, Phys. Rev. Lett. **55**, 2028 (1985).
[6]H. Ohtani, R. J. Wilson, S. Chiang, and C. M. Mate, Phys. Rev. Lett. **60**, 2398 (1988).
[7]Ph. Avouris and R. Wolkow, Phys. Rev. Lett. **60**, 1049 (1988).
[8]U. K. Köhler, J. E. Demuth, and R. J. Hamers, Phys. Rev. Lett. **60**, 2499 (1988).
[9]J. K. Glimzewski, B. Reihl, J. H. Coombs, and R. R. Schlitter, J. Phys. B **72**, 497 (1988).
[10]P. Muralt and D. Pohl, Appl. Phys. Lett. **48**, 514 (1988).
[11]P. K. Hansma, B. Drake, O. Marti, J. A. Gould, and C. B. Prater, Science **243**, 641 (1989).
[12]Y. Martin, D. W. Abraham, and H. K. Wickramasinghe, Appl. Phys. Lett. **52**, 1103 (1988).
[13]G. Binnig, C. F. Quate, and Ch. Gerber, Phys. Rev. Lett. **56**, 930 (1986).
[14]Y. Manassen, R. J. Hamers, J. E. Demuth, and A. J. Castellano, Jr., Phys. Rev. Lett. **62**, 2531 (1989).
[15]D. Shachal and Y. Manassen, Phys. Rev. B **44**, 11 528 (1991).
[16]D. Shachal and Y. Manassen, Phys. Rev. B **46**, 4795 (1992).
[17]A. W. McKinnon, M. E. Welland, T. Rayment, and M. H. Levitt (unpublished).
[18]Y. Nishi, Jpn. J. Appl. Phys. **10**, 52 (1971).
[19]W. Krieger, T. Suzuki, M. Völcker, and H. Walther, Phys. Rev. B **41**, 10 229 (1990).
[20]W. Rohrbeck, E. Chila, H. Fröhlich, and J. Reidel, Appl. Phys. A **52**, 344 (1991).
[21]G. Binnig, N. Garcia, H. Rohrer, J. M. Soler, and F. Flores, Phys. Rev. B **30**, 4816 (1984).
[22]S. N. Moltokov, Surf. Sci. **264**, 235 (1992).